Deep-Sea Research, Vol. 29, No. 7A, pp. 883 to 892, 1982.
Printed in Great Britain.

0198-0149/82/070883-10 $03.00/0

INSTRUMENTS AND METHODS

Temporal and spatial resolution of pump sampling systems

D. L. MACKAS* and R. W. OWEN†

(*Received* 11 *June* 1981; *final revision received* 4 *January* 1982; *accepted* 4 *January* 1982)

Abstract—A simple empirical method is described for determining the fine-scale resolution of continuous flow-through sampling systems. An input delta function is provided by injection of fluorescent dye into the sampler intake. The output fluorescent signal provides time-domain estimates of delay and signal spread; Fourier transformation of the output provides the frequency domain transfer function of the system. Systems with direct intakes (hose or through-hull fitting) can resolve features of 30-s duration or less; however, sea chest intakes cause substantial blurring of the input signal. Attempts to increase vertical spatial resolution by slow lowering rates can result in profiles characterized by apparent micropatchiness and multiple layering, artifacts of the procedure.

INTRODUCTION

CONTINUOUS flow sensors are now widely used to sample spatial and temporal distributions in aquatic environments. Variables measured include temperature, salinity, chlorophyll fluorescence, dissolved nutrients, and particle abundance (LORENZEN, 1966; KELLEY, WHITLEDGE and DUGDALE, 1975; STEELE and HENDERSON, 1977; PUGH, 1978; DENMAN and MACKAS, 1978). The primary motivation for continuous sampling is the potential for much finer resolution than can be achieved by discrete sampling methods. In particular, the understanding of small-scale features and processes (e.g., plankton patchiness, fronts, and vertical layering) is almost totally dependent on the resolution, accuracy, and interpretability of continuous measurements.

Although the useful sample density obtainable from flow-through sensors is large, it is finite. Optimum resolution and analytical efficiency are achieved only by an appropriate matching of digitizing interval, instrument response time(s), rate of movement of the sampler intake, and scales of spatial and temporal variability of the quantity being mapped. Both slow instrument response and mixing of sample water in the supply plumbing (if present) attenuate high-frequency components of the data and give a smoothed time series relative to the sampled system. Such attentuation has both beneficial and adverse effects. On the positive side, it allows slightly longer intervals between digitizing of the incoming data (see the discussion of aliasing in PLATT and DENMAN, 1975). Conversely, measurement at scales

* Institute of Ocean Sciences, Sidney, B.C. V8L 4B2, Canada.
† Southwest Fisheries Center, National Marine Fisheries Service, La Jolla, CA 92038, U.S.A.

overlapping into the zone of attentuation may be essential for many applications; the smoothed output data will then result in underestimation of small-scale gradients and, if the data are eventually expressed in spectral form, will impose an artificial truncation of the high frequency or high wavenumber end of the estimated variance spectrum.

In this article we describe a method for measuring the effective cut-off frequency of a flow-through sampling system and present data and response spectra for several pump systems. We then show how the time-scale cut-off can impose severe constraints on both spatial and temporal sampling of rapidly varying data. We also show that published examples of vertical micro-patchiness (e.g., STRICKLAND, 1968) may be artifacts resulting from internal wave displacements past a slowly descending sample intake.

METHODS

Calculation of response spectra and selection of input signals

Except that the relevant time scales are substantially longer, the analysis is exactly equivalent to that conventionally applied to linear electronic systems. JENKINS and WATTS (1968) provided a development from which we extract the following important points:

The output $u(t)$ of a 'physically realizable' system can be expressed as a weighted integration over all prior inputs

$$y(t) = \int_0^\infty h(u)x(t-u)\,du, \tag{1}$$

where $x(t)$ is the input function and $h(u)$ is the weighting coefficient at time lag u. [The only constraint is that $h(u)$ must not itself vary significantly during the measurement.] The complex frequency spectrum of the output is $Y(f)$ and is the Fourier transform of the output series

$$Y(f) = \int_{-\infty}^{\infty} y(t)e^{-i2\pi ft}\,dt, \tag{2}$$

where f is a frequency expressed in cycles per unit time. The output spectrum is also equal to the product of the spectra of input and weighting functions

$$Y(f) = H(f) \cdot X(f), \tag{3}$$

where

$$H(f) = \int_0^\infty h(u)\,e^{-i2\pi fu}\,du \tag{4}$$

and

$$X(f) = \int_{-\infty}^{\infty} x(t)\,e^{-i2\pi ft}\,dt. \tag{5}$$

The 'power spectrum' $|Y(f)|^2$ is the squared modulus of $Y(f)$ [i.e., if $Y(f) = a\cos(f) + ib\sin(f)$ then $|Y(f)|^2 = a^2 + b^2$]. It partitions the variance of the time series $Y(t)$ among the contributing frequency scales [see JENKINS and WATTS (1968) or PLATT and DENMAN (1975) for more detailed development and for equivalent equations corresponding to finite series length and discrete sampling intervals]. Because the expected frequency

dependence of the power spectrum can be derived for stochastic processes such as turbulent diffusion, data on oceanographic distributions are commonly reduced to this form (PLATT and DENMAN, 1975).

For our purposes, the input function $x(t)$ is the data field being sampled (one realization of a random process), $|X(f)|^2$ is the power spectrum we would like to estimate (assumed to be statistically representative of the random process under study), $y(t)$ is the output observed from the instrument, and $|Y(f)|^2$ is the corresponding observed power spectrum. Finally, $H(f)$ is the combined transfer function of the sampling system plumbing and the sensing instrument, and $|H(f)|^2$ is the squared gain function, relating the magnitude of the output variance to the magnitude of the input variance within each frequency band. Conveniently, an input function which is a 'spike' at one sampling point and zero elsewhere (an impulse or delta function), has a power spectrum that is constant with frequency. The output time series resulting from this input is equal to a constant multiple of the time domain weighting function $h(u)$ plus a small (one hopes) measurement error $e(t)$. The output power spectrum $|Y(f)|^2$ is proportional to the squared gain spectrum plus the noise spectrum due to instrument drift. jitter, and quantizing error.

$$|Y(f)|^2 = |H(f)|^2 \cdot |X(f)|^2 + |\varepsilon(f)|^2, \tag{6}$$

where $|\varepsilon(f)|^2$ is the noise power spectrum and can be estimated from the output spectrum of a constant (or better, a slowly and linearly varying) input. The estimated 'true' spectrum is therefore

$$|X(f)|^2 = \frac{|Y(f)|^2}{|H(f)|^2} - |\varepsilon(f)|^2. \tag{7}$$

In practice, both $Y(f)$ and $H(f)$ normally become small relative to $\varepsilon(f)$ at large f and the usefulness of a reconstructed input spectrum is questionable.

If the input spike is sufficiently strong to make the measurement error $e(t)$ very small relative to the output signal $y(t)$, the input and output series can be treated as deterministic functions rather than as realizations of random processes. The ensemble or frequency band averaging conventionally applied in spectral analysis of random data is therefore unnecessary, and the transfer function can be estimated to sufficient accuracy directly from the discrete Fourier transform of the digitized output signal. Many computer programs are available for this task; we used the Waveform Analysis Pac available for the Hewlett–Packard HP-85 desk-top computer.

Sampling system—sensors and water supply

The data and analyses reported here correspond to five different but reasonably typical flow-through sampling configurations. In each, the final component is a portable instrument package (MACKAS, LOUTTIT and AUSTIN, 1980) consisting of a bubble trap, a resistive particle counter, a Turner Designs fluorometer, and an Applied Microsystems Ltd. temperature and conductivity sensor (all connected in series). For convenience of measurement and because it has the slowest response time of the various sensors, we used the output signal from the fluorometer for our analyses. The 'impulse' input function was a syringe of fluorescent dye (a dilute solution of Rhodamine B in seawater), which a SCUBA diver injected quickly (<1 s) into the initial seawater intake. The total system response was invariably slow relative to the manufacturer-specified (and observed) time constant of the fluorometer, implying that the observed high-frequency attentuation was dominated by mixing within the supply system. On

this basis, we have accepted the system plus fluorometer gain function as a slightly conservative but adequate model for all sensors in the system. Other applications might require independent evaluation for each of several sensors (for example, an AutoAnalyzer® might have both longer lag time and considerably greater internal smoothing of the sample signal). Output of the fluorometer was recorded continuously on a paper strip chart from which the data were digitized at time intervals short relative to the rate of output signal variation (range 2 to 30 s, depending on the supply system).

Five different supply plumbing configurations (A to E) were examined. System A is used for vertical profiling and consists of a submerged intake hose (35 m long, 3.25 cm i.d.), a deck mounted Moyno progressive cavity pump, and 20 m of 2 cm i.d. hose leading to the instrument package. The pump output is 1.25 l s^{-1}, of which 25% is passed through the sensors and the remainder discharged overboard. B to E are the scientific seawater supply systems on four local research vessels and are used for horizontal mapping of near-surface distributions. The pump intake for E lies within a recessed sea chest (vol. 2 m^3), which also provides cooling water for the ship's engines. The outer wall of the sea chest is a flush-mounted grating of about 50% porosity, and the dye spike was injected through this grating. Although the ship was stationary during the test, its engines were run in neutral at cruising speed to approximate normal flow rates through the sea chest. The remaining systems (B, C, and D) have direct intake through the hull. B and C have relatively short runs (10 to 15 m) of internal supply piping, while D has a run of nearly 40 m. All of the ships' systems provided flows of 0.19 to 0.25 l s^{-1} to the sensor package.

RESULTS

Time domain representation of sampling system resolution

Output time series for the various pump-and-plumbing systems are shown in Fig. 1a to e. Two estimates of signal modification are presented in the figure. Delay is the mean lag time in seconds for arrival of the fluorescent tracer and is given by:

$$\text{Delay} = \frac{\sum_{i=1}^{N} F_i i\Delta t}{\sum_{i=1}^{N} F_i}, \tag{8}$$

where F_i is the fluorescence of the ith digitized point, Δt is the digitizing interval in seconds, and N is the number of sampling intervals from dye injection to final disappearance of the output pulse. This Delay statistic will normally be equal to the mean residence time of water in the system (system volume divided by flow rate) provided the tracer moves with the flow so that there is no chromatographic separation of tracer and carrier. The appropriate use of this statistic is to align the data output with the record of sample location. FWHA (full width at half amplitude) is a measure of the broadening of the <1-s input pulse and is the time between upward and downward crossings of $F_i = 0.5\, F_{max}$. This is an estimate of the temporal resolution (as opposed to the phase shift) imposed by the sampling system and is also useful as a guide to the sampling frequency needed to avoid possible aliasing errors.

The following features should be noted from the figure: First, although Delay and FWHA are obviously correlated, the correlation is imperfect and their numerical values are con-

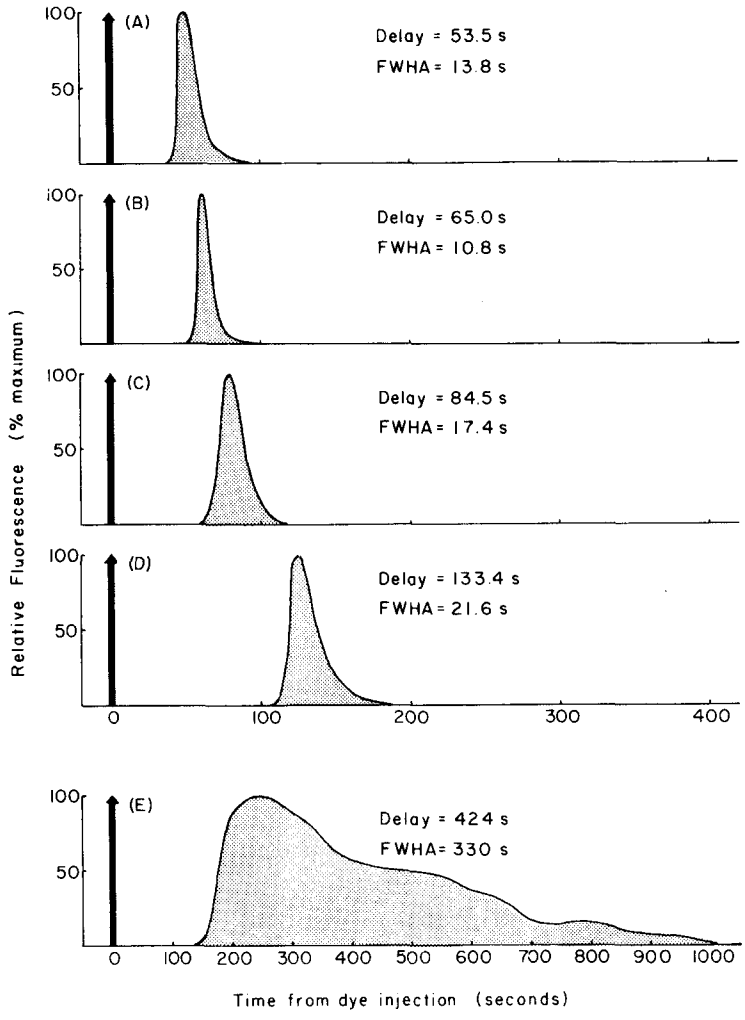

Fig. 1. Input (arrow) and output (stippled) signals for injection of fluorescent dye into five pump sampling systems. A is a vertical profiling system, B to D are ships' seawater supplies with direct intakes through the hull, and E (note scale change along time axis) is a ship's supply with intake drawing from a semi-enclosed sea chest. See text for details and definition of Delay and FWHA statistics.

siderably different; FWHA is normally much smaller than Delay. Information will therefore be lost from the output signal if the data logging interval is set to match the mean residence time of the system (a fairly common practice, see e.g., STEELE and HENDERSON, 1977). Second, the output is characteristically skewed, with mean delay time being longer than the delay to $F_i = F_{max}$. Third, system E (sample drawn from the sea chest) has delay and pulse width that are extremely large compared to the other systems. In addition, there are indications with this system of multiple decaying output pulses (possibly caused by a slow rotational circulation within the sea chest).

Frequency domain representation of sampling system resolution

Fourier transformation of the output signals from the various sampling systems gives the power spectra shown in Fig. 2. The spectra have been normalized to a maximum value of unity at the lowest frequency band. The effect of this normalization is to depict the squared gain function for each system; an 'observed' power spectrum calculated from a data series will be the within-frequency-band product between the 'true' spectrum (specifically that for a single realization from the underlying random process) and the squared gain spectrum of the system used to collect the data.

The optimum form for the above gain spectrum is rectangular; unity for all frequencies below the Nyquist frequency $(2\Delta t)^{-1}$ and zero for all higher frequencies. However, the measured spectra all show a more gradual transition into a roll-off region in which the squared gain varies approximately as the inverse square of frequency. In system E the roll-off commences at very low frequencies indicating strong attenuation of variability at all scales shorter than about 10^3 s (the spectral peak at 0.003 cycles s^{-1} represents the periodicity of the multiple output pulses mentioned in the previous section). The remaining four sampling systems are much more similar in their spectra and are characterized by higher corner frequencies and more rapid and uniform roll-off. The half-power points fall at time scales (cycle lengths) of 54.1, 40.8, 68.5, and 90.9 s for systems A to D, respectively. These time scales are approximately four times the corresponding FWHA estimates and are extremely well correlated with them ($r^2 = 0.996$ vs 0.836 for the correlation with Delay). To a good approximation, a discrete sampling interval roughly equal to the FWHA time scale both eliminates potential aliasing and records nearly all of the information passed by the sampling system. The investigator can use these data in their raw recorded form but should note that both time and frequency domain data have been attenuated at the shortest time scales included in the analysis. Alternately, the investigator can resort to a more elaborate procedure of digitally filtering the data to give a more rectangular frequency response function and a better match between corner and the final effective sampling frequencies (see e.g., BENDAT and PIERSOL, 1971).

Implications for spatial resolution

The most common application of continuous flow sensors lies in sampling of spatial variation rather than purely temporal variation. For studies of near-surface horizontal variability, the sampler intake is towed from or attached to a ship moving at a speed of 2 to 10 knots (roughly 1 to 5 m s^{-1}). Systems A to D all show good resolution of features having greater than about 30-s duration; their equivalent spatial resolution (at easily obtained ship's speeds) can therefore be set between 30 and 150 m, which is adequate for many purposes. (A more severe limitation is usually found at the other end of the sampling scale, i.e., the maximum distance a ship can travel within a time scale that can reasonably be described as synoptic.) Somewhat finer spatial resolution can be obtained by reducing in size or eliminating the bubble trap (vol. 10 l), but smaller scales are in general more effectively sampled by *in situ* sensors. In contrast, the spatial scale for system E is 0.65 to 3.4 km, which would be too coarse for description of sharp and frequently encountered gradients such as frontal boundaries.

Pump sampling systems can impose more severe restrictions when used for studies of vertical distributions. Vertical gradients in the ocean are substantially stronger than horizontal gradients; significant changes in concentration often occur over vertical distances of 1 to 5 m or less. This suggests that resolution of such features is best achieved by lowering the sample

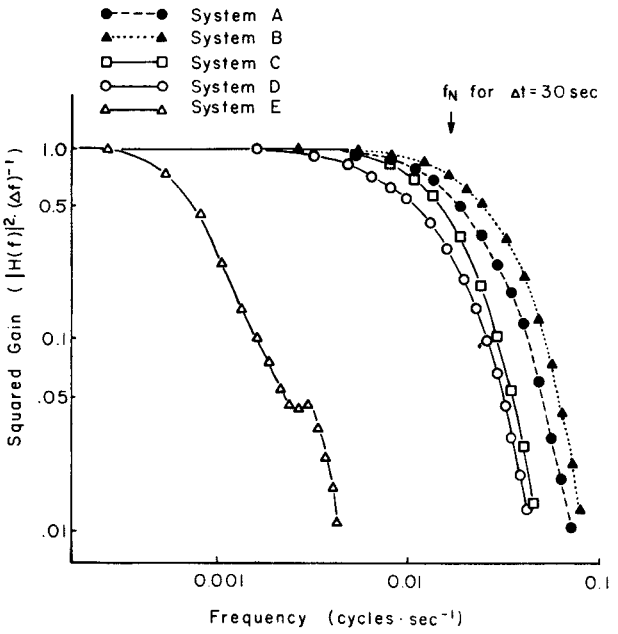

Fig. 2. Squared gain spectra (output variance vs frequency) for the five sampling systems. Small arrow labelled f_N indicates the maximum frequency detected by a 30-s discrete sampling interval.

intake slowly (e.g., 1 to 2 m min^{-1} or slower). However, as noted by HOLLIGAN (1978), this is potentially misleading because the vertical structure can experience internal wave or turbulent displacements that are substantially more rapid than 1 m min^{-1}, and the desired 'snapshot' can easily become a 'multiple exposure'.

To illustrate the above problem, we present simulated results of slow vertical profiling through a water column perturbed by internal gravity waves. The internal wave displacement is modeled as a solitary wave in a two-layer fluid with the lower layer substantially thicker than the upper (BENJAMIN, 1966). Input parameters are selected to approximate water properties and wave amplitudes observed off La Jolla, California (LAFOND and COX, 1962; MULLIN and BROOKS, 1972). The vertical distribution of chlorophyll is simulated by superposition of a Gaussian chlorophyll maximum centered on the pycnocline, a nearly uniform upper layer concentration, and an asymptotic approach to zero below the pycnocline. Equations for the profile are:

$$\mathrm{Chl}(\eta) = A + Be^{-(\eta-P)^2/S^2} \quad \text{for} \quad \eta \leqslant P \tag{9}$$

and

$$\mathrm{Chl}(\eta) = Ae^{-C(\eta-P)} + Be^{-(\eta-P)^2/S^2} \quad \text{for} \quad \eta > P, \tag{10}$$

where η is the depth at which the sampled stratum would be in the absence of internal wave displacement and is calculated from the sampling depth $Z(t)$ and the displacement $F(\eta, t)$; P is the pycnocline depth (also in the undisturbed water column); and $A = 2.5$, $B = 5$, $S = 3$, and $C = 0.25$ are constants respectively determining the upper layer concentration, the concentration within and vertical thickness of the sub-surface maximum, and the exponential rate of decrease of concentration below the pycnocline. Figure 3 shows a time vs depth section of

the displacement of vertical structure caused by passage of the internal wave, and three possible sampling trajectories through the structure (1 m min^{-1} lowering speed through an unperturbed water column, 1 m min^{-1} intersecting the wave trough, and 4 m min^{-1} intersecting the wave trough). Figure 4 a to c shows the corresponding simulated profiles of chlorophyll concentration. Samples from a non-wavy region (Fig. 4a) accurately portray the estimated chlorophyll distribution. However, in the presence of even a solitary internal wave, the sampler may sample the same water two or more times at different depths (Fig. 3; see also PINGREE, HOLLIGAN and HEAD, 1977; HAURY, BRISCOE and ORR, 1979). This produces (Fig. 4b) an apparent chlorophyll profile characterized by spurious fine-scale peaks and troughs. The exact profile (number and intensity of the apparent peaks) depends on the interaction between lowering rate; starting time of the profile; phase, speed, and amplitude of the wave(s); and width and location of the chlorophyll maximum. However, the simulated profiles bear a disturbing resemblance to the multiple-peaked fluorometric profiles reported by STRICKLAND (1968) off La Jolla. These and similar profiles (e.g., BERMAN, 1972; KIEFER and AUSTIN, 1974; KIEFER and LASKER, 1975) have been interpreted as evidence for fine-scale vertical patchiness that is missed by conventional sampling with water bottles at standard depths. Although such an interpretation is at least partially valid in that to produce such highly structured profiles there must be a narrow stratum with markedly higher (or lower)

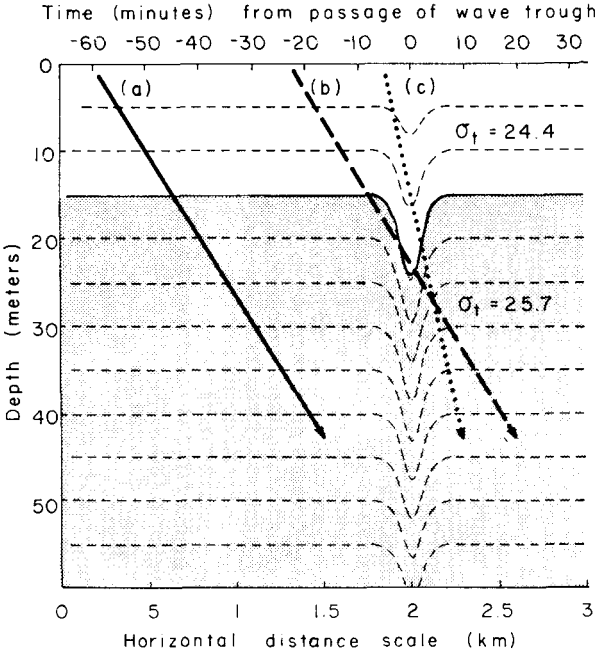

Fig. 3. Simulated internal wave displacements in a two-layer water column. Upper layer is 15 m thick when undisturbed and has density corresponding to water of 18°, 33.8 x 10^{-3} salinity. Lower layer extends to bottom at 120 m and has density corresponding to 12°C, 33.8 x 10^{-3}. Wave amplitude is 10 m at the interface and wave speed is 0.51 m s^{-1}. Dashed lines indicate the variation of displacement trajectories as a function of depth. Three sampling trajectories through the wave structure are shown. Solid line a is 1 m min^{-1} lowering speed through an undisturbed water column. Broken line b is 1 m min^{-1} intersecting the trough. Dotted line C is 4 m min^{-1} intersecting the trough.

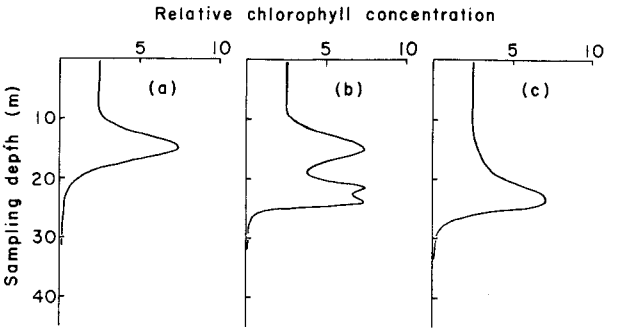

Fig. 4. (a, b, c) Simulated chlorophyll profiles for the three sampling trajectories shown in Fig. 3. See text for equations describing the form of the undistorted profile.

chlorophyll concentration, the multiple layering may be entirely an artifact of the sampling procedure. We suggest two procedural options for eliminating this possible artifact from studies of vertical microdistribution. One is to make the sampling more synoptic. This can be done either by using a specialized microsampler to obtain simultaneous discrete samples at closely spaced depths (OWEN, 1981), by rapid lowering of a fast-response *in situ* sensor (if available), or by greatly increasing the lowering rate of the pump intake (and engineering a reduced FWHA time scale to maintain the needed spatial resolution). Figure 4c shows the more accurate profile obtained within the wave trough using a four-fold increase in simulated lowering rate. A second option is to include as part of the pump profiling system sensors for physical variables (temperature, conductivity, and from these salinity and density). If correction is made for temperature offset produced within the sampling system, an independent 'fast' profile of the physical structure (e.g., by a concurrent CTD cast) can then be used to define a density vs depth chart onto which the remaining pump profile variables can be plotted (DENMAN and HERMAN, 1978; MACKAS, BOYD, SMITH and SANTANDER, 1981). This approach has the added advantage that the upper cut-off frequency for internal wave perturbations can be estimated from the data, and the lowering rate altered to suit individual sampling locations. Distortion of the profile will normally be minimal if the lowering rate is set to be greater than about twice the product of the buoyancy frequency (converted to cycles per unit time) and the local wave amplitude (usually 10 to 20 m or less for relatively high frequency and near-surface internal waves).

Acknowledgements—We wish to thank Drs K. L. DENMAN, D. M. FARMER, and R. E. THOMSON for their comments and discussions.

REFERENCES

BENDAT J. S. and A. G. PIERSOL (1971) *Random data: analysis and measurement procedures*. Wiley, Interscience, New York, 407 pp.

BENJAMIN T. B. (1966) Internal waves of finite amplitude and permanent form. *Journal of Fluid Mechanics*, **25**, 241–270.

BERMAN T. (1972) Profiles of chlorophyll concentrations by *in vivo* fluorescence: some limnological applications. *Limnology and Oceanography*, **17**, 616–618.

DENMAN K. L. and A. W. HERMAN (1978) Space-time structure of a continental shelf ecosystem measured by a towed porpoising vehicle. *Journal of Marine Research*, **36**, 693–714.

DENMAN K. L. and D. L. MACKAS (1978) Collection and analysis of underway data and related physical measurements. In: *Spatial pattern in plankton communities*, J. H. STEELE, editor, Plenum Press, New York, pp. 85–109.

HAURY L. R., M. G. BRISCOE and M. H. ORR (1979) Tidally generated internal wave packets in Massachusetts Bay. *Nature*, **278**, 312–317.

HOLLIGAN P. M. (1978) Patchiness of subsurface phytoplankton populations of the northwest European continental shelf. In: *Spatial pattern in plankton communities*, J. H. STEELE, editor, Plenum Press, New York, pp. 221–238.

JENKINS G. M. and D. G. WATTS (1968) *Spectral analysis and its applications*. Holden-Day, San Francisco, California, 525 pp.

KELLEY J. C., T. E. WHITLEDGE and R. C. DUGDALE (1975) Results of sea surface mapping in the Peru upwelling system. *Limnology and Oceanography*, **20**, 784–794.

KIEFER D. A. and R. W. AUSTIN (1974) The effect of varying phytoplankton concentration on submarine light transmission in the Gulf of California. *Limnology and Oceanography*, **19**, 55–64.

KIEFER D. A. and R. LASKER (1975) Two blooms of *Gymnodinium splendens*, an unarmored dinoflagellate. *Fishery Bulletin*, **73**, 675–678.

LAFOND E. C. and C. S. COX (1962) Internal waves. In: *The sea*, Vol I, M. N. HILL, editor, Wiley, Interscience, New York, pp. 731–763.

LORENZEN C. J. (1966) A method for the continuous measurement of *in vivo* chlorophyll concentration. *Deep-Sea Research*, **13**, 223–227.

MACKAS D. L., C. M. BOYD, S. SMITH and H. SANTANDER (1981) Vertical distributions of plankton in the upper 35 m of the Peruvian upwelling zone: application of a shipboard electronic plankton counting system. *Boletin Instituto del Mar del Peru*, vol. extr. (ICANE), 67–71.

MACKAS D. L., G. C. LOUTTIT and M. J. AUSTIN (1980) Spatial distribution of zooplankton and phytoplankton in British Columbia coastal waters. *Canadian Journal of Fisheries and Aquatic Sciences*, **37**, 1476–1487.

MULLIN M. M. and E. R. BROOKS (1972) Vertical distribution of juvenile *Calanus* and phytoplankton within the upper 50 m of water off La Jolla, California. In: *Biological oceanography of the northern North Pacific Ocean*, A. Y. TAKENOUTI, editor, Idemitsu Shoteu, Tokyo, pp. 347–354.

OWEN R. W. (1981) Microscale patchiness of small plankton on the Chimbote Shelf, Peru, *Boletin Instituto del Mar del Peru*, vol. extr. (ICANE), 274–279.

PINGREE R. D., P. M. HOLLIGAN and R. N. HEAD (1977) Survival of dinoflagellate blooms in the western English Channel. *Nature*, **265**, 266–269.

PLATT T. and K. L. DENMAN (1975) Spectral analysis in ecology. *Annual Review of Ecology and Systematics*, **6**, 189–210.

PUGH P. R. (1978) The application of particle counting to an understanding of the small-scale distribution of plankton. In: *Spatial pattern in plankton communities*, J. H. STEELE, editor, Plenum Press, New York, pp. 111–129.

STEELE J. H. and E. W. HENDERSON (1977) Plankton patches in the northern North Sea. In: *Fisheries mathematics*, J. H. STEELE, editor, Academic Press, New York, pp. 1–19.

STRICKLAND J. D. H. (1968) A comparison of profiles of nutrient and chlorophyll concentrations taken from discrete depths and by continuous recording. *Limnology and Oceanography*, **13**, 388–391.